IOP Conf. Series: Materials Science and Engineering **114** (2016) 012133 doi:10.1088/1757-899X/114/1/012133

A hybrid joint based controller for an upper extremity exoskeleton

Ismail Mohd Khairuddin[1], Zahari Taha[1], Anwar P.P. Abdul Majeed[1], Abdel Hakeem Deboucha[1], Mohd Azraai Mohd Razman[1], Abdul Aziz Jaafar[1] and Zulkifli Mohamed[2]

[1]Faculty of Manufacturing Engineering, Universiti Malaysia Pahang, 26600 Pekan, Pahang, Malaysia
[2]Faculty of Mechanical Engineering, Universiti Teknologi MARA, 40450 Shah Alam, Selangor, Malaysia

E-mail: ismailkhai@ump.edu.my

Abstract. This paper presents the modelling and control of a two degree of freedom upper extremity exoskeleton. The Euler-Lagrange formulation was used in deriving the dynamic modelling of both the human upper limb as well as the exoskeleton that consists of the upper arm and the forearm. The human model is based on anthropometrical measurements of the upper limb. The proportional-derivative (PD) computed torque control (CTC) architecture is employed in this study to investigate its efficacy performing joint-space control objectives specifically in rehabilitating the elbow and shoulder joints along the sagittal plane. An active force control (AFC) algorithm is also incorporated into the PD-CTC to investigate the effectiveness of this hybrid system in compensating disturbances. It was found that the AFC-PD-CTC performs well against the disturbances introduced into the system whilst achieving acceptable trajectory tracking as compared to the conventional PD-CTC control architecture.

1. Introduction

The life expectancy of amongst the elderly around the globe has increased over the past two decades [1]. In Malaysia, approximately 8.3% of its population is above 60 years old [1-2]. The Malaysian Ministry of Health's 2013 annual report disclosed that the number of stroke patients increases at an average of 300% annually [3]. It is common that individuals that fall into the aforementioned statistics are affected with partial or complete loss of motor control on upper-limb which essentially compromises their activities of daily living [4].

Continuous and repetitive rehabilitation activities allow these individuals to relearn the best possible use of their limbs and regain their mobility [4-6]. However, traditional rehabilitation therapy is regarded to be too costly and laborious which in turn limiting rehabilitation activities of the patients [4-6]. The drawbacks of traditional rehabilitation methods have led the research community at large in employing robotics to mitigate the present predicament.

Robotic exoskeletons or simply exoskeletons are mechanical structures that consists of several mechanisms which resembles the human limb. Exoskeletons in the case of upper limb rehabilitation are designed to operate seamlessly with the human upper limb [7]. Active research on upper limb exoskeletons for rehabilitation has been reported in the literature. A nonlinear sliding mode control strategy was applied on a 2 degrees of freedom (DOF) ExoRob that tracks the trajectory of the elbow

and forearm [8]. A proportional-integral-derivate (PID) controller was also for trajectory tracking of a 5 DOF upper limb exoskeleton [9]. An intelligent control method was employed by Aiguo et al. to a 4 degrees of freedom exoskeleton [10]. Fuzzy Logic was coupled with a proportional-derivative (PD) control technique for trajectory tracking of the exoskeleton.

The proposed study aims at examining the joint tracking performance of a simple yet robust control strategy namely AFC-PD based computed torque control (CTC) of a two DOF upper limb exoskeleton system. The system is designed to rehabilitate the flexion/extension of the elbow and the adduction/abduction of the shoulder joint in the sagittal plane. The system will be then subjected to two different type of disturbance (constant and harmonic) to investigate its compensation performance. The performance of the proposed control strategy will be then compared to the conventional PD-CTC controller by taking into consideration same operating conditions. This study in novel, as the proposed control architecture has yet been employed in any upper limb exoskeleton system.

2. Dynamics of Upper Extremity

Figure 1 depicts the upper-extremity dynamics of the human limb and exoskeleton that are modelled as rigid links joined by joints. The two-link model restricted at the sagittal plane and the human-machine interaction is assumed to be seamless. Furthermore, the frictional elements that act on both the exoskeleton and human joints, as well as other unmodelled variables, are also ignored.

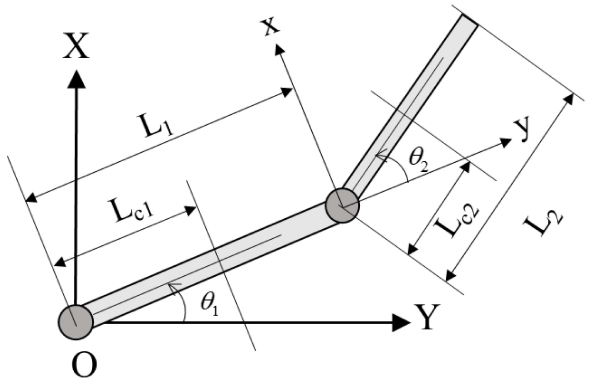

Figure 1. The two-link manipulator that resembles the human upper limb.

In figure 1, the subscripts 1, and 2 represents the parameters of the first link (upper arm), and the second link (forearm), respectively. L is the length segments of the limb and exoskeleton; L_c is the length segments of the limb as well as the exoskeleton about its centroidal axis and θ is the angular position of the links. The Lagrangian formulation is employed in deriving the equation of motions for the non-linear dynamic system. The upper-extremity dynamics of the coupled nonlinear differential equations may be written in the following standard form [11]

$$\boldsymbol{\tau} = \mathbf{D}(\theta)\ddot{\theta} + \mathbf{C}\left(\theta,\dot{\theta}\right) + \mathbf{G}(\theta) + \boldsymbol{\tau}_d \tag{1}$$

where $\boldsymbol{\tau}$ is the actuated torque vector, $\mathbf{D}$ is 2 × 2 inertia matrix of the exoskeleton and limb, $\mathbf{C}$ is the Coriolis and centripetal torque vector, $\mathbf{G}$ is the gravitational torque vector whilst $\boldsymbol{\tau}_\mathbf{d}$ is the external disturbance torque vector. The matrix form of equation (1) may be written as

$$\begin{bmatrix}\tau_1\\ \tau_2\end{bmatrix} = \begin{bmatrix}D_{11} & D_{12}\\ D_{21} & D_{22}\end{bmatrix}\begin{bmatrix}\ddot{\theta}_1\\ \ddot{\theta}_2\end{bmatrix} + \begin{bmatrix}C_{11} & C_{12}\\ C_{21} & C_{22}\end{bmatrix}\begin{bmatrix}\dot{\theta}_1\\ \dot{\theta}_2\end{bmatrix} + \begin{bmatrix}G_1\\ G_2\end{bmatrix} + \begin{bmatrix}\tau_{d1}\\ \tau_{d2}\end{bmatrix} \tag{2}$$

where the components of the inertial matrix, Coriolis components and gravitational terms are

$$D_{11} = m_1 L_{c1}^2 + J_1 + m_2\left(L_1^2 + L_{c2}^2 + 2L_1 L_{c2}\cos\theta_2\right) + J_2 \tag{3}$$

$$D_{12} = D_{21} = m_2 L_1 L_{c2} \cos\theta_2 + m_2 L_{c2}^2 + J_2 \tag{4}$$

$$D_{22} = m_2 L_{c2}^2 + J_2 \tag{4}$$

$$C_{11} = -2m_2 L_1 L_2 \dot{\theta}_2 \sin\theta_2 \tag{4}$$

$$C_{12} = -m_2 L_1 L_2 \dot{\theta}_2 \sin\theta_2 \tag{4}$$

$$C_{21} = m_2 L_1 L_2 \dot{\theta}_1 \sin\theta_2 \tag{4}$$

$$C_{22} = 0 \tag{4}$$

$$G_1 = (m_1 + m_2) g L_1 \cos\theta_1 + m_2 g L_2 \cos(\theta_1 + \theta_2) \tag{4}$$

$$G_2 = m_2 g L_2 \cos(\theta_1 + \theta_2) \tag{4}$$

where m is the combination of mass, whilst J is mass moment of inertia of the exoskeleton as well as the limbs, respectively, and g is the gravitational acceleration taken as 9.81 m/s^2. The anthropometric parameters of human segments used in this study was adopted from [12]. The remaining parameters are listed in section 4.

3. Control Architecture

Hewit and Burdess introduced the notion of AFC that is based on the principle of invariance and Newton's second law of motion in the early eighties [13]. Mailah and co-researchers has extended the effectiveness of this control strategy by incorporating intelligent methods in approximating the inertial matrix of the dynamic system. The accurate approximation of the estimated inertial mass is crucial as it triggers the disturbance compensation effect of the controller [14-17]. This control architecture has been effectively demonstrated both numerically as well as experimentally in a number of different applications [14-17]. The schematic of the PD-CTC-AFC strategy is depicted in figure 2. The hybrid control scheme is only activated upon the trigger of the AFC loop, without its initiation the system is controlled by the traditional PD-CTC control scheme.

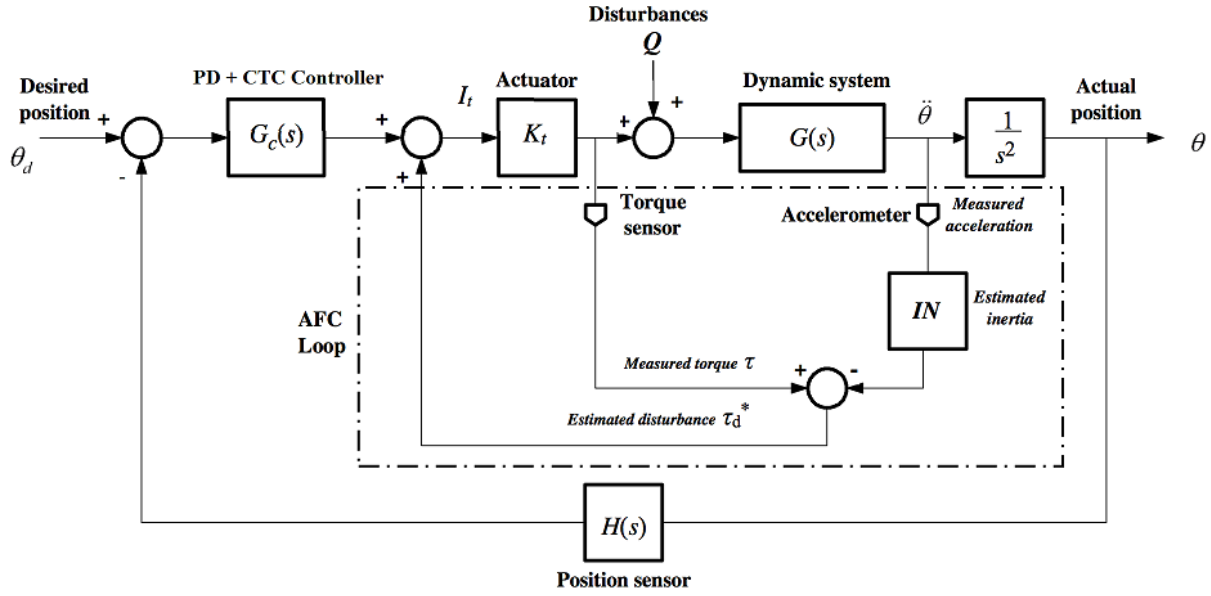

Figure 2. The PD-CTC with AFC scheme for the control of the upper limb exoskeleton system.

The torque is generated by the feedback linearisation control law viz. PD-CTC. A detail elaboration on the mechanism of this control law is well discussed in the literature [11]. The PD-CTC control architecture is often expressed as [11].

$$\boldsymbol{\tau} = \mathbf{D}\left(\ddot{\theta}_d + K_p(\theta_d - \theta) + K_v(\dot{\theta}_d - \dot{\theta})\right) + \mathbf{C}\left(\theta, \dot{\theta}\right) + \mathbf{G}\left(\theta\right) \tag{4}$$

where, $\dot{\theta}_d$ and $\dot{\theta}$ are the desired and present angular velocities, respectively, whilst θ_d and θ are the desired and present angular positions, respectively. K_d and K_p are the derivative and proportional constants, respectively. In order to compensate the actual disturbances τ_d , the estimated disturbance torque , τ_d^* has to be calculated. The estimated disturbance torque, τ_d^* may be expressed through the following equation

$$\tau_{\mathrm{d}}{}^{*} = \tau - \mathbf{IN}\ddot{\theta} \tag{4}$$

where $\ddot{\theta}$ is the measured acceleration signal, **IN** is the estimated inertial matrix, whilst τ is the measured applied control torque.

In this study, the determination of the estimated inertial matrix was acquired by means of crude approximation technique. Previous studies have shown that this method is adequate as long as the **IN** chosen lies within certain bounds of the actual inertial matrix, **D** [18]. The estimated inertial matrix, **IN** may be computed form the following equation

$$[\mathbf{IN}] = \mathrm{k} * [\mathbf{D}] \tag{4}$$

where k is a constant bounded between 0.4 < k < 1.2. The off-diagonal terms of the matrix are ignored whilst the diagonal terms are retained. In this study, the suitable value of k was found to be 0.4.

4. Simulation

In this study, the simulation works were performed in MATLAB and Simulink. The simulation parameters employed in this study are as follows

Upper-limb parameters:
Limb and exoskeleton robot lengths: L_1 = 0.34 m, L_2 = 0.25 m;
Centre of mass: L_{c1} = 0.17 m, L_{c2} = 0.125 m;
Forearm and upper arm masses: $m_{upperarm}$ = 1.91 kg, $m_{forearm}$ = 1.22 kg;
Exoskeleton masses: m_{exo1} = 0.34 kg, m_{exo2} = 0.25 kg;

Mass moment of inertia of limb: J_{limb1} = 0.2374 kg.m^2, J_{limb2} = 0.0873 kg.m^2;
Mass moment of inertia of exoskeleton: J_{exo1} = 0.0131 kg.m^2, J_{exo2} = 0.0052 kg.m^2;

Controller parameters:
Controller gains (heuristically acquired):
K_{p1} = 1 000, K_{d1} = 90;
K_{p2} = 1 000, K_{d2} = 90;

Diagonal elements of estimated inertia matrix:
$\mathbf{IN}_1$ = 0.2935 kg.m^2, $\mathbf{IN}_2$ = 0.0.0743 kg.m^2.

Simulation parameters:
Integration algorithm: ode2 (Heun)
Simulation start time: 0.0
Simulation stop time: 10 sec
Fixed-step size: 0.001

5. Result and Discussion

Figures 3 to 5 illustrate the results obtained through the simulation study. The results demonstrates the performance of the proposed controller performing the trajectory of a sinusoidal input with an amplitude of 45° (0.7855 rad) on both the elbow and shoulder joints under three different conditions; without disturbance (figure 3), constant disturbance with an amplitude of 100 N.m. (figure 4) and a harmonic disturbance with an amplitude of 500 and frequency 1 rad/s (figure 5).

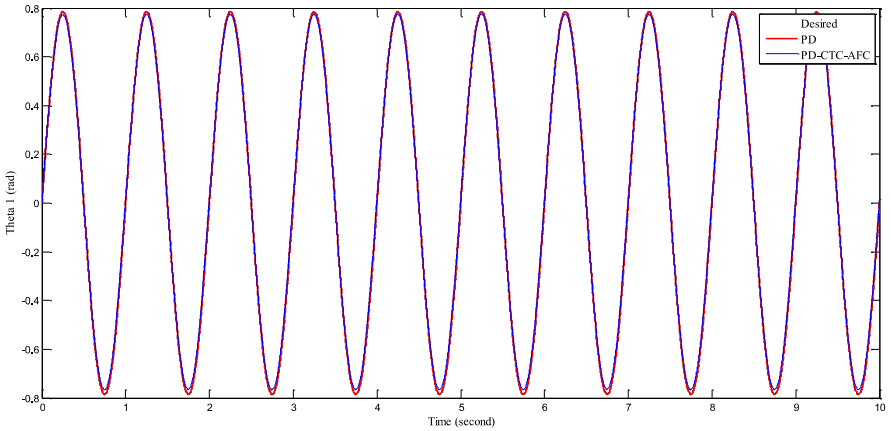

Figure 3(a). Result of joint 1 angle trajectory without any disturbance.

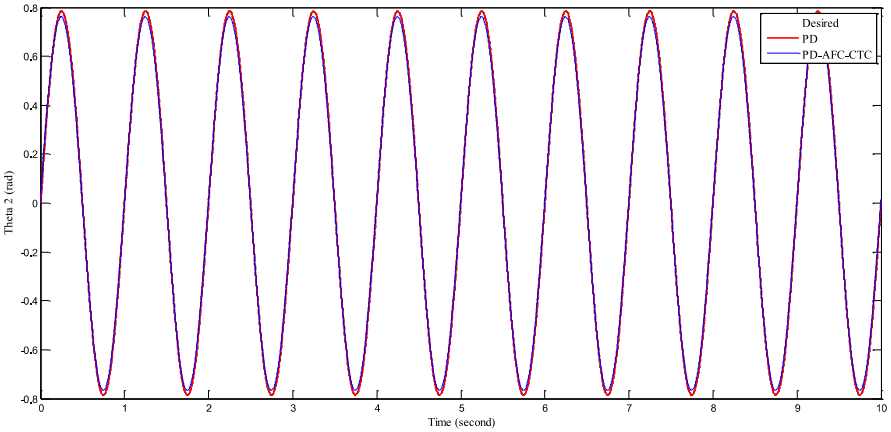

Figure 3(b). Result of joint 2 angle trajectory without any disturbance.

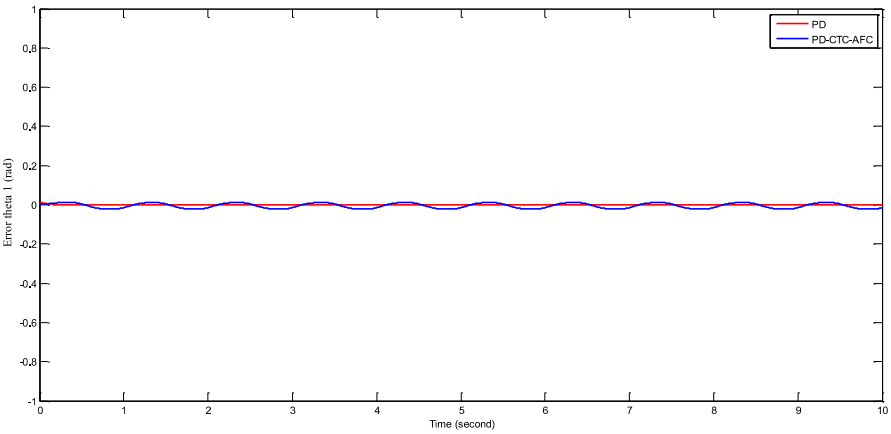

Figure 3(c). Tracking error of joint 1 without any disturbance.

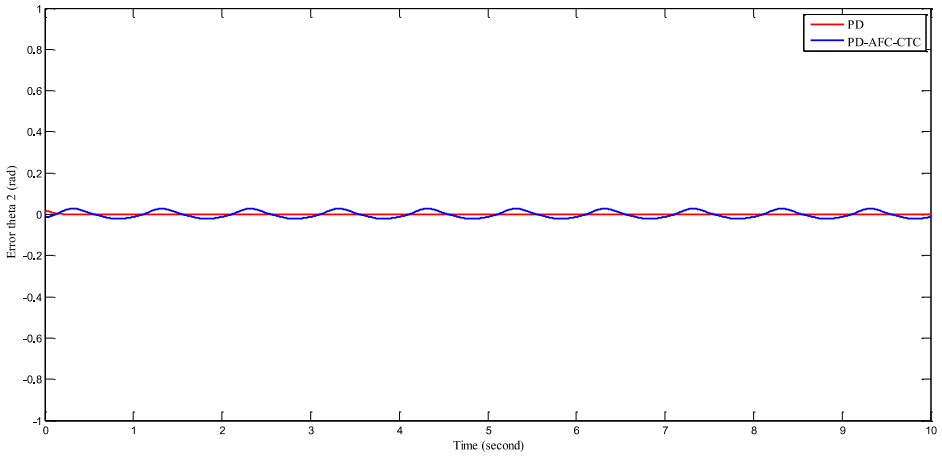

Figure 3(d). Tracking error of joint 2 without any disturbance.

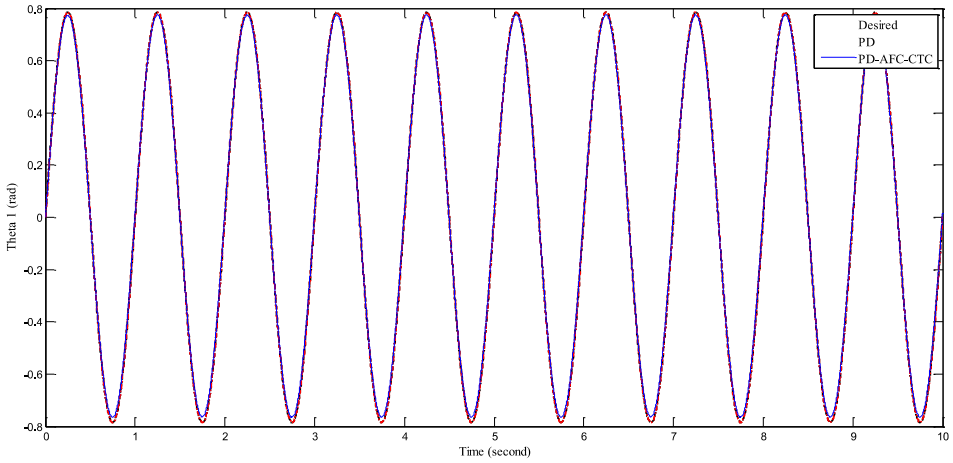

Figure 4(a) Result of joint 1 angle trajectory with a constant disturbance of 100 N.m.

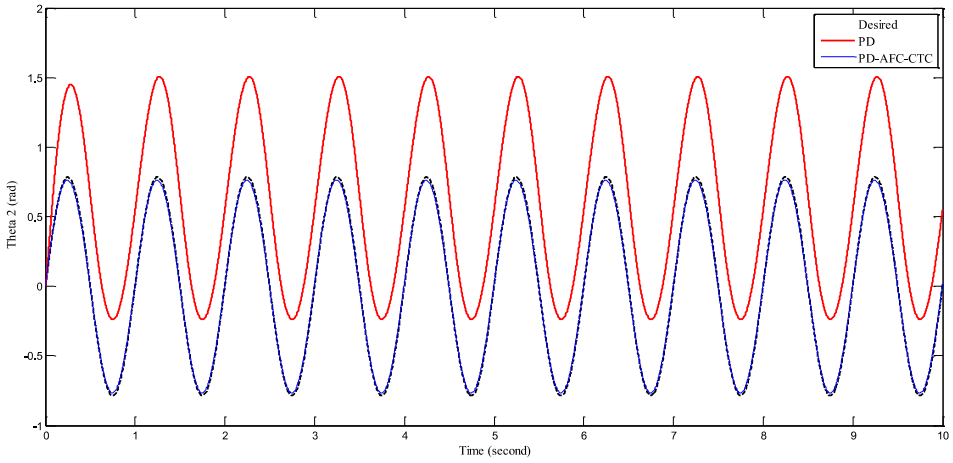

Figure 4(b). Result of joint 2 angle trajectory with a constant disturbance of 100 N.m.

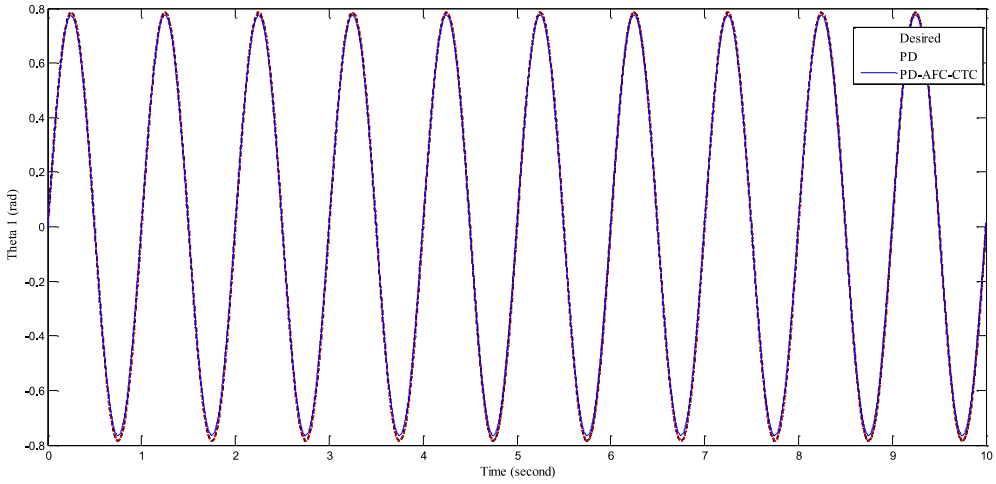

Figure 5(a). Result of joint 1 angle trajectory with a harmonic disturbance of 500 N.m.

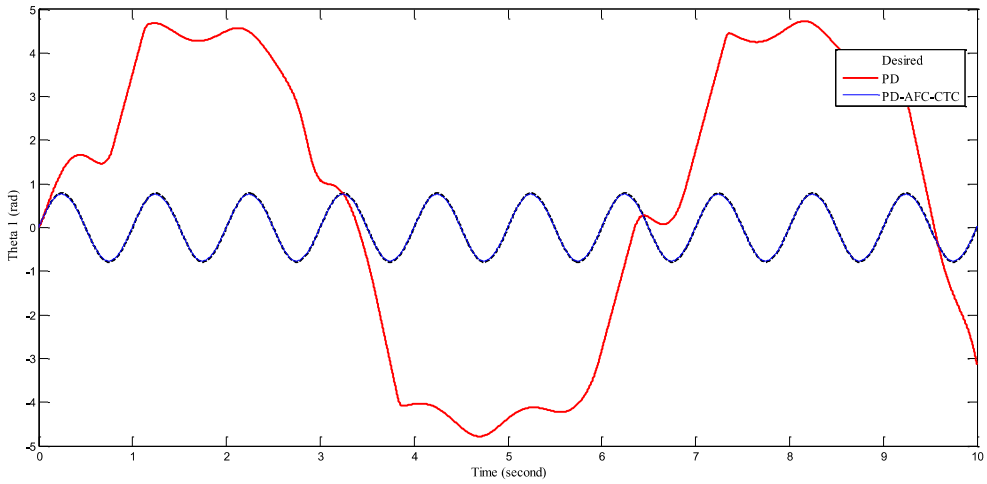

Figure 5(b). Result of joint 2 angle trajectory with a harmonic disturbance of 500 N.m.

Table 1. Summary of joint root mean square tracking error ($error_{RMS}$).

	Elbow joint, θ_1 $error_{RMS}$ (rad)		Shoulder joint, θ_2 $error_{RMS}$ (rad)	
Disturbance Type	PD-CTC	PD-CTC-AFC	PD-CTC	PD-CTC-AFC
None	895.619 μ	13.557 m	1.398 m	16.869 m
Constant (100 N.m.)	903.756 μ	13.557 m	616.544 m	16.869 m
Harmonic (500 N.m.)	898.571 μ	13.557 m	3.404	16.860 m

The root mean square error ($error_{RMS}$) of both joints are listed in Table 1. It is apparent that the PD-CTC control scheme provides the best trajectory tracking for both joints without the influence of any form of disturbance. However, as the system is subjected to disturbances, the conventional PD-CTC strategy suffer considerably, particularly at joint 2. Conversely, the PD-CTC-AFC rejects both types of disturbance well at joint 2, whilst providing acceptable trajectory tracking with an $error_{RMS}$ of approximately 2% at both joints. It is noteworthy to mention that the CTC architecture relies on

accurate modelling of the system to ensure its efficacy in performing trajectory tracking [11]. Therefore, in practical application, the inclusion of the AFC loop shall assist the CTC in treating the unmodelled dynamics as a form of disturbances. This in turn, will make the system more robust whilst ensuring acceptable trajectory tracking. Furthermore, by incorporating intelligent mechanisms in estimating the inertial matrix may provide a better estimation of the inertial matrix that in turn would yield better disturbance compensation and even better trajectory tracking.

6. Conclusion

It is evident from the study that although the conventional PD-CTC control strategy provides excellent joint trajectory tracking without the presence of disturbance as compared to the proposed PD-CTC-AFC. The latter performs reasonably well even under the influence of external disturbances. The study further suggests the effectiveness of the proposed controller, especially in treating unmodelled dynamics which is prevalent in real environment. It can also be concluded with its relatively small tracking error the proposed control scheme is suitable for practical implementation on an upper limb exoskeleton for early stage rehabilitation. Further investigation may be carried out by enhancing the present proposed system incorporating intelligent methods in attaining suitable estimated inertial parameters.

References

[1] World Health Organization 2014 *World Health Statistics*
[2] Taha Z, Majeed A P P A, Tze M Y W P and Rahman A G A 2015 *J. Med. Bioeng.* **4** 1
[3] Ministry of Health Malaysia 2013 *Annual Report 2013*
[4] Lo H S and Xie S Q 2012 *Med. Eng. Phys*. **34** 261-8
[5] Volpe B T, Ferraro M, Krebs H I and Hogan N 2002 *Curr. Atheroscler. Rep.* **4** 270–6
[6] Loureiro R C V, Harwin W S, Nagai K and Johnson M 2011 *Med. Biol. Eng. Comput.* **49** 1103–18
[7] Cannan James and Hu Huosheng 2012 *Technical Report.* **CES 518**
[8] Rahman M.H, Saad M, Kenne J.P, and Archambault P.S 2010 *Proc., Conf on. Control and Automation (Morocco)*
[9] Liang Guangye, Ye Wenjun and Xie Qing 2012 *Proc Conf on Control (China)*
[10] Song Aiguo, Xu Guozheng and Li HuiJun 2011 *Advance Robotics.***25** 229-251
[11] Craig J J 2005 Introduction to Robotics: Mechanics and Control (Upper Saddle River: Pearson Prentice Hall)
[12] Veeger H E J, Yu B, An K N and Rozendal R H 1997 *J. Biomech.* **30** 647–52
[13] Hewit J and Burdess J 1981 *Mech. Mach. Theory.* **16** 535–42
[14] Jahanabadi H, Mailah M, Zain M Z M and Hooi H M 2011 *J. Bionic. Eng.* **8** 474–84
[15] Noshadi A and Mailah M 2012 *Sci. Iran* **19** 132–41.
[16] Mailah M, Pitowarno E and Jamaluddin H 2006 *Int. J. Adv. Robot. Syst.* **2** 125–34.
[17] Ramli H, Meon M S, Mohamed T L T, Isa A A M and Mohamed Z 2012 *Procedia Eng.* **41** 1389–97.
[18] Mailah M, Hewit J R and Meeran S 1996 *J. Mek.* **2** 52–68